



PERGAMON

Quaternary Science Reviews 20 (2001) 583–589



The phase relations among atmospheric CO₂ content, temperature and global ice volume over the past 420 ka

Manfred Mudelsee*

Institute of Meteorology, University of Leipzig, Stephanstr. 3, D-04103 Leipzig, Germany

Abstract

The phase relations (leads/lags) among atmospheric CO₂ content, temperature and global ice volume are key to understanding the causes of glacial–interglacial (G–IG) climate transitions. Comparing the CO₂ record with other proxy variables from the Vostok ice core and stacked marine oxygen isotope records, allows the phase relations among these variables, over the last four G–IG cycles, to be estimated. Lagged, generalized least-squares regression provides an efficient and precise technique for this estimation. Bootstrap resampling allows account to be taken of measurement and timescale errors. Over the full 420 ka of the Vostok record, CO₂ variations lag behind atmospheric temperature changes in the Southern Hemisphere by 1.3 ± 1.0 ka, and lead over global ice-volume variations by 2.7 ± 1.3 ka. However, significant short-term changes in the lag of CO₂ relative to temperature, subsequent to Terminations II and III, are also detected. © 2001 Elsevier Science Ltd. All rights reserved.

1. Introduction

Earth's climate in the Late Pleistocene is dominated by large fluctuations in the amount of ice stored on the continents. The ice accumulates gradually over time whereas it decays more abruptly, in a glacial “termination”, the period of such a sawtooth-shaped glacial–interglacial (G–IG) cycle amounting to approximately 100 thousand years (ka) (Broecker and van Donk, 1970). Also other variables internal to the climate system, such as atmospheric carbon dioxide and temperature, exhibit sawtooth-shaped cycles in the Late Pleistocene (Petit et al., 1999). Major external forcing of Pleistocene G–IG cycles are variations of the Earth's orbit which determine the geographical distribution of received solar insolation (Milankovitch's explanation, substantiated by Hays et al. (1976)). However, the role of internal variables, which have a potential for an own forcing of G–IG cycles or may be involved in feedback mechanisms, is currently not clearly understood (Broecker and Henderson, 1998). Therefore, the phase relations (leads/lags) among these variables — atmospheric CO₂ content, temperature and global ice volume — are key to understanding the causes of G–IG climate transitions.

The ice core from Vostok (Petit et al., 1999) in Antarctica provides an important record of atmospheric CO₂ concentration (measured on enclosed air bubbles), extending back in time 420 ka, which encompasses the last four G–IG cycles. It also provides a high-resolution record of the ice's deuterium excess (δD), which is a proxy for air temperature over the Vostok site. Furthermore, oxygen-isotopic composition of air in the Vostok core ($\delta^{18}O_{\text{air}}$) can be used as an indicator of global ice volume (Sowers et al., 1991).

Previous estimates of the phase relations among atmospheric CO₂, temperature and ice volume, based on studies of ice cores from both Greenland and Antarctica (Sowers et al., 1991; Raynaud et al., 1993; Li et al., 1998), relied on marine oxygen isotope records ($\delta^{18}O_{\text{mar}}$) such as the SPECMAP stack (Martinson et al., 1987), or the stack of Bassinot et al. (1994), as proxies for global ice volume. According to these studies, it seems that, over the last 150 to 200 ka, variations in Vostok's CO₂ record lag behind changes in atmospheric temperature, but lead over changes in global ice volume.

A major problem with such comparisons is the unknown accuracy of the estimated lags. The time series analysed generally exhibit measurement noise, and also the conservativeness (quality) of the proxies used is not perfect. A larger contribution to the estimation error possibly arises from uncertainties associated with the age models used. Various assumptions were made in their construction and they are not exact, especially in the

* Tel.: + 49-(0)341-97-32866; fax: + 49-(0)341-97-32899.
E-mail address: mudelsee@rz.uni-leipzig.de (M. Mudelsee).

earlier part of the record (before, say, Termination II, about 127 ka before present).

This paper specifically addresses the problem of determining the accuracy of estimating the phase relations between Vostok's CO_2 and proxy air-temperature and ice-volume records for the past 420 ka, by means of a precise statistical estimation technique (lagged GLS regression). The results obtained take into account both measurement and age-model errors. Also, short-term changes in lag are analysed.

2. Materials and methods

The ice core from Vostok in Antarctica (location: 78°S , 106°E) provides the following records (Petit et al., 1999) of Late Pleistocene climate: δD of ice (Fig. 1(a), in ‰ deviation with respect to standard mean ocean water), a proxy for air-temperature changes over the Vostok site (Petit et al., 1999); CO_2 content of enclosed air bubbles (Fig. 1(a)), a good proxy for the atmospheric content of this greenhouse gas (Raynaud et al., 1993); and $\delta^{18}\text{O}_{\text{air}}$ of enclosed air bubbles (Fig. 4(a), in ‰ deviation with respect to modern air composition), a proxy for global ice-volume changes (Sowers et al., 1991). The GT4 time-scale (Petit et al., 1999) for the Vostok core was derived by means of an ice-flow model. The core covers the past 420 ka. It is important to note that the ice-age is not identical to the air-age at the same core depth (Barnola et al., 1991).

The deep-sea sediment core MD900963 from the Indian Ocean provides a record of $\delta^{18}\text{O}_{\text{mar}}$ (Fig. 3a, in ‰ deviation with respect to the NBS standard and measured on shells of benthic foraminifera), a proxy for global ice-volume changes (Bassinot et al., 1994). SPEC-MAP is a stacked record of $\delta^{18}\text{O}_{\text{mar}}$ (planktonic foraminifera), constructed from five geographically distributed deep-sea cores (Imbrie et al., 1984; Martinson et al., 1987). Both records MD900963 and SPEC-MAP have orbitally tuned timescales.

The lagged polynomial regression (Li et al., 1998) is illustrated using Vostok's δD record, for which a parabolic model was found to be suitable:

$$y_u = a + bx_{t+l} + cx_{t+l}^2 + \varepsilon, \quad (1)$$

where y is atmospheric CO_2 , u the Vostok's air-age, x the interpolated δD and t the Vostok's ice-age. The regression parameters are a , b , c and, notably, l , the time lag. A positive value for l means that there is a lead of CO_2 over δD . The error, ε , is serially dependent (Robinson, 1977) with autocorrelation time, τ_y , because preliminary examinations with ordinary least-squares regression indicated persistence. Therefore, generalized least squares (GLS), which takes persistence into account, offers a more precise estimation (Sen and Srivastava, 1990). Since τ_y is unknown, GLS regressions are carried out

over a range of τ_y values (first loop). In order to find the best lag, l is varied (in 0.005 ka increments) in a second loop. The final solution is taken from the regression which yields the minimal reduced sum of squares, χ_v^2 .

Lagged GLS regression is a more efficient method than comparing dates of events (e.g., the start of Termination II) because its estimation is based on all data points of the time series.

3. Results

3.1. CO_2 versus δD

Fig. 1 shows the result of the lagged regression of Vostok's δD record on its CO_2 record. Fig. 1(a) reveals clearly that the number of deuterium measurements

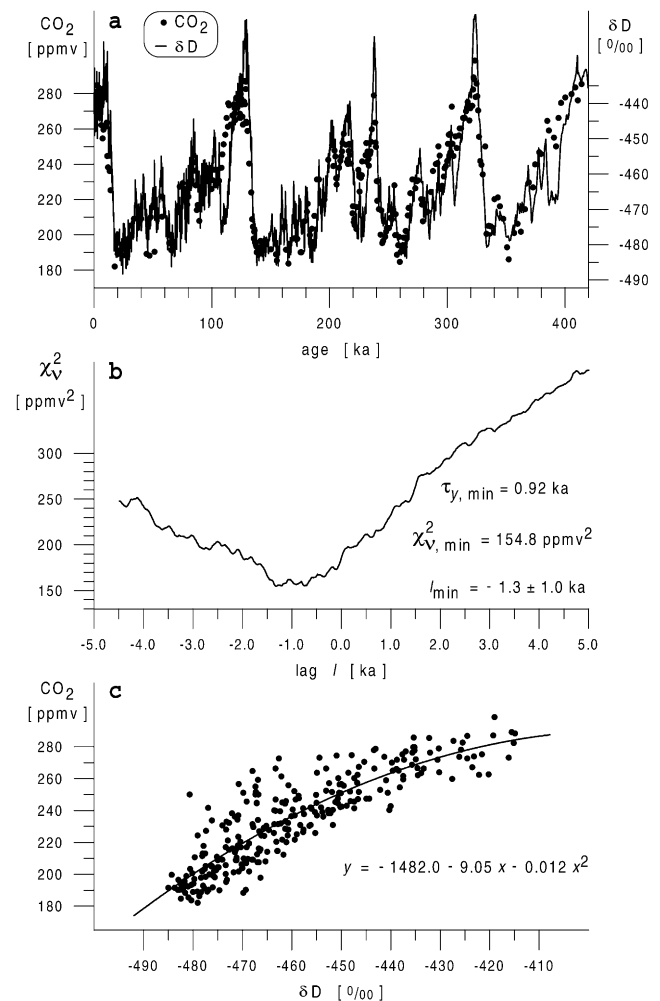


Fig. 1. Lagged regression of Vostok's δD on Vostok's CO_2 . (a) Time series, both on the GT4 timescale (Petit et al., 1999). (b) Reduced sum of squares in dependence on the lag. τ_y is the GLS autocorrelation time. Subscript "min" denotes the best fit result. (c) Lagged parabolic GLS regression.

(3311) is much larger than the number of CO₂ measurements (283), which makes the error introduced by the interpolation (Eq. (1)) negligible. The parabolic regression model was found to be better than a linear model which has a slightly higher χ^2_v . This is reflected by the lower kurtosis (greater flatness) of the distribution of the CO₂ data in comparison with the δD data. The result is a lag of 1.3 ka of CO₂ behind δD . Subtracting the regression line (Fig. 1c) from the y -data gives the residuals. These showed no temporal trend. Also, experiments with extracted time intervals confirmed that no significant long-term change in phase occurred over the last 420 ka.

Parametric bootstrap simulations (Efron and Tibshirani, 1993) provided the $1 - \sigma$ error for the estimated lag. That is, the measurement and timescale errors for both time series (y, u, x, t) are modelled to produce a pair of simulated time series. Lagged regression is repeated, yielding a value l^* . A total of 2000 such pairs was produced to suppress simulation noise (Efron and Tibshirani, 1993). The median of l^* can be compared with the estimated value for l to evaluate possible estimation bias. For all of the lagged regressions carried out, no significant bias was detected. Instead of the standard deviation of l^* , the value $1.4826 \text{ mad}(l^*)$ is used here, where mad is the median of absolute distances from median(l^*) (e.g. Tukey, 1977). This error ($1 - \sigma$ because of the normalization) is more robust against non-normal distributions of l^* .

In the case of CO₂ versus δD , simulated y and x followed the measurement errors (Petit et al., 1999) which are 2.5 ppmv CO₂ and 1.0‰ δD (reported as upper limits). In order to simulate u , the sedimentation rate at Vostok, S , was used, which varies with a relative error of 14% around its general trend (Fig. 2). Simulated S trans-

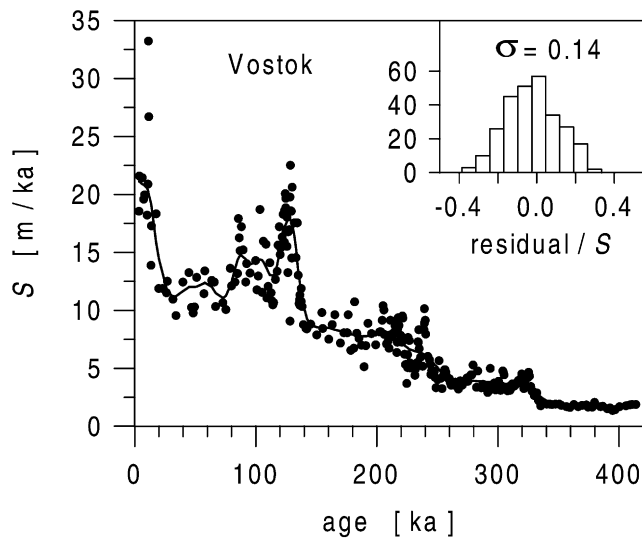


Fig. 2. Sedimentation rate S at Vostok. The raw data (●) result from the age-depth distribution of the CO₂ data. The trend (heavy line) is an adaptive kernel smoothing (Herrmann, 1997). The distribution of the residuals (inset) indicates a relative error of S of 14%.

formed Vostok depth into a simulated u sequence. This sequence was further compressed or expanded to fit into the GT4 timescale error range (Petit et al., 1999), which is ≤ 5 ka for the last 110 ka; ≤ 10 ka for “most of the record” (here assumed to be 110–300 ka); and ≤ 15 ka in the early part. (These upper limits were used because they constitute the most conservative estimates.) This technique takes into account the two aspects of the uncertain timescale: span, and distribution of points over the span. Simulated t (Vostok’s ice-age) had to depend on simulated u (Vostok’s air-age). Actually, only the uncertainty in ice-age/air-age difference had to be superimposed, which is about 1 ka (Petit et al., 1999). Sensitivity experiments with other values confirmed that this uncertainty is the main contribution to the error of the estimated lag of CO₂ behind δD : $l = -1.3 \pm 1.0$ ka.

3.2. CO₂ versus $\delta^{18}O_{\text{mar}}$

Fig. 3 shows the result of the lagged linear regression of the $\delta^{18}O_{\text{mar}}$ record from deep-sea sediment core MD900963, on Vostok’s CO₂ record. On an average, a CO₂ data point is separated from its corresponding $\delta^{18}O_{\text{mar}}$ point by about 0.7 ka. This is clearly less than the estimation uncertainty which makes the interpolation error negligible. Over the whole age interval, linear GLS regression gave only a moderate fit ($\chi^2_v = 251.7 \text{ ppmv}^2$). The parabolic model was no better. However, the residuals exhibit a clear temporal trend, that is, between 420 and 196 ka, variations in CO₂ seem to lag behind those of $\delta^{18}O_{\text{mar}}$, whereas, from 150 ka to present, they lead. The dates were determined with the trend-analysing program RAMPFIT (Mudelsee, 2000). This subdivision (early/recent interval) improved the fit (Fig. 3b). Furthermore, by omitting the CO₂ points between 112 and 120 ka, the fit for the recent interval ($l = 6.2 \pm 2.7$ ka, $\chi^2_v = 127.4 \text{ ppmv}^2$) was improved considerably (Fig. 3b). These “outliers” (Fig. 3c), detected by residual analysis, are discussed in Section 4.

The bootstrap simulations for $x = \delta^{18}O_{\text{mar}}$ used the reported measurement error (Bassinot et al., 1994) of 0.05‰. Simulations of the marine timescale, t , were also done via modelling the sedimentation-rate uncertainty. Bassinot et al. (1994) gave an age error of 5 ka which was adopted. Since u and t are not interdependent in the case of CO₂ versus $\delta^{18}O_{\text{mar}}$, the bootstrap simulations for u and t had to be independent, leading to larger estimation uncertainties. Note that these uncertainties (2.7 ka and 3.7 ka) are still smaller than the adopted age error, which is due to the serial correlation of a timescale. (That is, if, for a given depth in a core, the true age is larger than its nominal age from the timescale, the true age for the neighbouring depth is likely to be also larger than its nominal value.) They still allow the statistical conclusion that a lag change occurred between 150 and 196 ka.

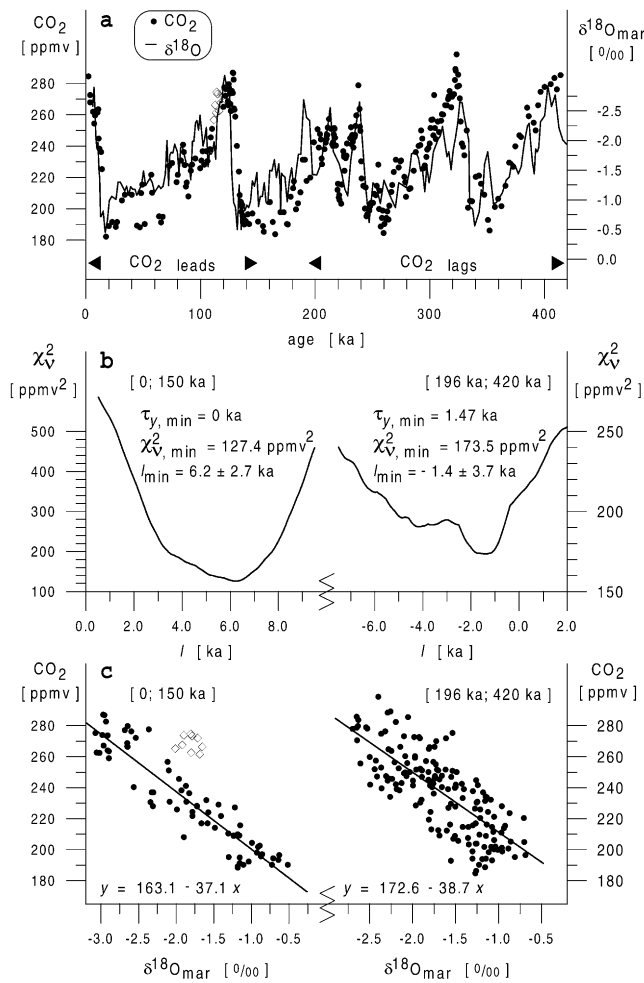


Fig. 3. Lagged regression of deep-sea sediment core MD900963's $\delta^{18}\text{O}_{\text{mar}}$ on Vostok's CO_2 . (a) Time series. $\delta^{18}\text{O}_{\text{mar}}$ is on an orbitally tuned timescale. CO_2 leads over $\delta^{18}\text{O}_{\text{mar}}$ in the recent interval (0–150 ka) and lags behind it in the early interval (196–420 ka). Outliers (\diamond) in the recent interval, between 110 and 120 ka, are determined in (c). See text for further details. (b) Reduced sum of squares in dependence on the lag (recent/early interval). (c) Lagged linear GLS regression (recent/early interval). The outliers (\diamond) deviate systematically and are excluded from the regression.

The lagged regression of the SPECMAP $\delta^{18}\text{O}_{\text{mar}}$ stack on Vostok's CO_2 record yielded a similar result: a significant lag change at around 200 ka, from $l = 3.7 \pm 2.8$ ka, in the early interval, to $l = -3.2 \pm 4.0$ ka in the recent interval. Again, the “outliers” between 112 and 120 ka were detected.

3.3. CO_2 versus $\delta^{18}\text{O}_{\text{air}}$

Fig. 4 shows the result of the lagged linear regression of Vostok's $\delta^{18}\text{O}_{\text{air}}$ record on its CO_2 record. On average, a CO_2 data point is separated from its corresponding $\delta^{18}\text{O}_{\text{air}}$ point by about 0.5 ka. This is comparable to the estimation uncertainty, which means that a small amount of interpolation error has to be considered. The best

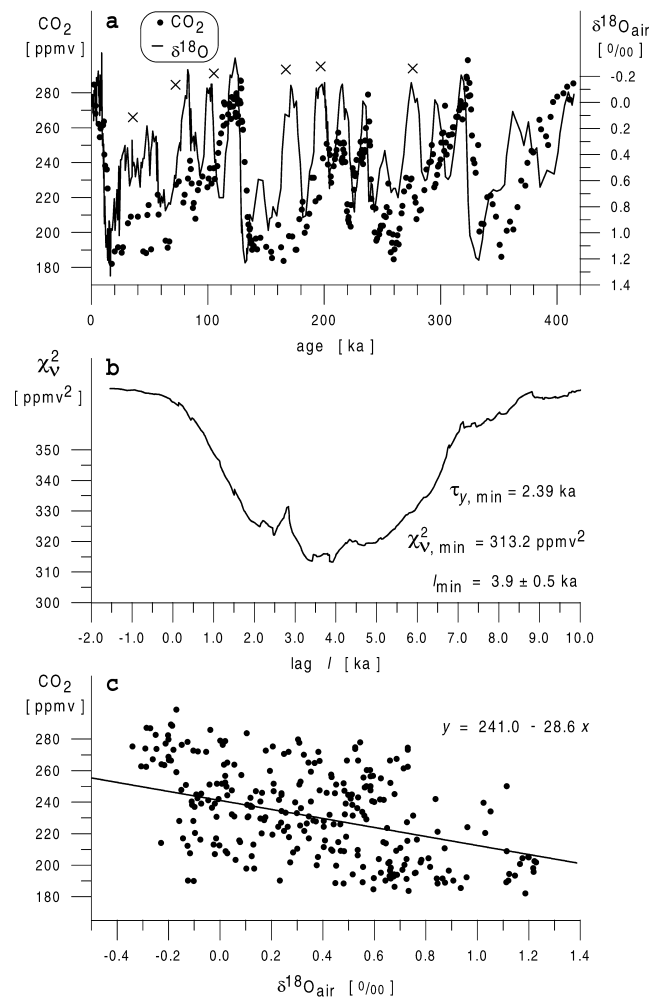


Fig. 4. Lagged regression of Vostok's $\delta^{18}\text{O}_{\text{air}}$ on Vostok's CO_2 . (a) Time series, both on the GT4 timescale. Crosses mark regions of systematic negative $\delta^{18}\text{O}_{\text{air}}$ deviations (see Section 3.3). (b) Reduced sum of squares in dependence on the lag. (c) Lagged linear GLS regression.

solution, a lead of CO_2 over $\delta^{18}\text{O}_{\text{air}}$ of 3.9 ka, has, in comparison with the other results (Figs. 1 and 3), a poor χ^2_V (313.2 ppmv²). This is reflected by the cloudy distribution of the regression points (Fig. 4(c)). The parabolic model did not perform any better. No long-term trend of the lag was detected. Residual analysis, and also visual inspection of Fig. 4(a), reveals the reason for the poor fit. The $\delta^{18}\text{O}_{\text{air}}$ curve shows considerable deviations from the general sawtooth shape which is common to the CO_2 , δD and $\delta^{18}\text{O}_{\text{mar}}$ curves (Figs. 1(a) and 3(a)). The regions of such deviations to negative $\delta^{18}\text{O}_{\text{air}}$ values are tentatively marked in Fig. 4(a).

The bootstrap simulations used a $\delta^{18}\text{O}_{\text{air}}$ measurement error of 0.1‰, which is a conservative estimate relative to the 0.075‰ reported by Malaizé et al. (1999). Because both CO_2 and $\delta^{18}\text{O}$ are measured on enclosed air, both u and t mean air-age and simulated u and t had

to be completely dependent, leading to a small uncertainty (0.5 ka) of the estimated lag.

3.4. CO₂ versus insolation

Lagged regressions on Vostok's CO₂ record were also carried out for two records of solar insolation (Berger and Loutre, 1991), mid-July at 65°N and mid-December at 90°S (results not shown). The linear as well as the parabolic regression model performed very poorly. The reason is the characteristic sawtooth shape of the CO₂ curve which is totally absent from any insolation curve (which is a mixture of sinusoids). More complicated regression tools, as they are given by mathematical models of palaeoclimate, would be necessary to infer the phase relation.

4. Discussion

The good fit of δD on CO₂ (Fig. 1) is remarkable because it means that the rather simple regression equation (1) parameterizing the relationship is valid over the last four G-IG cycles. $\sqrt{\chi^2_v} = 12.4$ ppmv is somewhat larger than the assumed CO₂ error, which can be explained by non-normal errors or an underestimation of the error (e.g., no gravitational correction was made). The result, $l = -1.3 \pm 1.0$ ka, is in excellent agreement with Sowers et al.'s (1991) result of -0.9 ± 0.8 ka. Their value resulted from analysing the 0–160 ka interval of the Vostok core. Although the uncertainty of the ice-age/air-age difference limits the accuracy (Section 3.1), a lag of CO₂ behind δD (Vostok temperature) seems to be very likely. This lag is constant on long timescales. To explore the possibility of short-term lag changes after a G-IG transition (Raynaud et al., 1993; Petit et al., 1999), a running window was employed, and the lag estimated using the CO₂ points inside the window (Fig. 5). A window width of 38 points (or 55 ka on average) was found to be a good compromise between the demand for many points contributing to the estimation and a high temporal resolution. A pronounced decrease to lag values of about -5 ka exists at around 85–120 ka, after Termination II, supporting previous results by Raynaud et al. (1993). The decrease to lag values of about -3 ka at around 220 ka, after Termination III, is significant. One should be cautious when interpreting results for the early part of the record because of the possibility of underestimated timescale errors (see below).

In the case of $\delta^{18}O_{\text{mar}}$ on CO₂ (Fig. 3), the simple linear regression model worked quite well. However, a subdivision into two intervals was necessary. The results for the recent interval (\leq about 150 ka), both from core MD900963 and from the SPECMAP stack, agree well with previous findings. Li et al. (1998) made a lagged regression of the SPECMAP $\delta^{18}O_{\text{mar}}$ stack on Vostok's

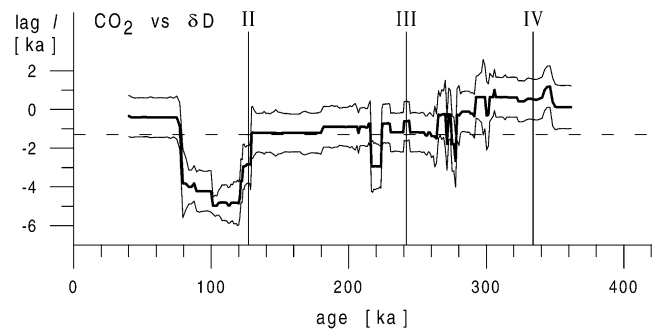


Fig. 5. Time-dependent lag (heavy solid line) between Vostok's CO₂ and δD , $1 - \sigma$ bootstrap error band (light solid lines) from 2000 simulations and, for comparison, the estimated lag for the full interval, 0 to 420 ka (dashed line). The running window for the estimation contains 38 points or 55 ka on average. The dates for the terminations (roman numerals) are from Bassinot et al. (1994).

CO₂ record (last 220 ka) and found $l = 4.5 \pm 1.5$ ka. This error value seems to be too small because of the timescale uncertainties. Nevertheless, the inferred lead of CO₂ over $\delta^{18}O_{\text{mar}}$ (global ice volume) appears to be certain. The value reported here, averaging the results from the investigated records, is $l = 5.0 \pm 1.9$ ka.

A different lag behaviour is exhibited by the “outliers” (Fig. 3) between 112 and 120 ka, on the recent side of the warm oxygen isotope substage 5e. When global ice volume was increasing from its minimum after Termination II, atmospheric CO₂ remained at a high level for about 8 ka. Such behaviour was not evident for the preceding terminations — possibly because of higher age uncertainties.

The results for the early interval (\geq about 200 ka) suggest a lag of CO₂ behind $\delta^{18}O_{\text{mar}}$ (global ice volume). However, the results from $\delta^{18}O_{\text{air}}$ from the Vostok core argue against this. The relatively poor fit of $\delta^{18}O_{\text{air}}$ on CO₂ (Fig. 4) can be explained by the Dole effect (hydrological cycle) which adds to the ice-volume signal of $\delta^{18}O_{\text{air}}$ (Sowers et al., 1991; Bender et al., 1994). The Dole effect might be responsible for the large, systematic negative deviations in the $\delta^{18}O_{\text{air}}$ record from the Vostok core (Fig. 4(a)). Removing the data from these intervals of the record improved the fit significantly, and gave nearly the same value for l . This substantiates the result: a lead of CO₂ over $\delta^{18}O_{\text{air}}$ by $l = 3.9 \pm 0.5$ ka. Malaizé et al. (1999) estimated the Dole effect by the difference $\delta^{18}O_{\text{air}} - \delta^{18}O_{\text{mar}}$. The attempt to subtract the Dole effect (estimated in this way) from $\delta^{18}O_{\text{air}}$ prior to the lag estimation would, therefore, lead to the result of Section 3.2 (CO₂ versus $\delta^{18}O_{\text{mar}}$)!

In order to calculate the lead of CO₂ over $\delta^{18}O_{\text{air}}$ -derived ice volume, the atmospheric turnover time of O₂ has to be subtracted. The reported values for that variable range between 1.2 ka (Bender et al., 1994) and 2–3 ka (Sowers et al., 1991). Using an average turnover time of 2 ± 1 ka yields the result that atmospheric CO₂ variations lead over global ice-volume variations by 1.9 ± 1.1 ka during the last 420 ka. This value of l is

somewhat smaller than the $\delta^{18}\text{O}_{\text{mar}}$ -derived value of 5.0 ka (recent interval), and also the values reported by Sowers et al. (1991) (4.3 ka) and Raynaud et al. (1993) (4–7 ka), both of whom analysed Termination II. These differences might be explained by relatively poor quality of fit (Fig. 4(c)) and some interpolation error. The weighted average value for l of 2.7 ± 1.3 ka, obtained from using $\delta^{18}\text{O}_{\text{mar}}$ (recent interval) and $\delta^{18}\text{O}_{\text{air}}$, might be closest to the true lag time for ice-volume changes following variations in atmospheric CO_2 content. On the other hand, as regards the interval before 200 ka, the $\delta^{18}\text{O}_{\text{air}}$ -derived estimate probably excludes the possibility of a negative value for l , as was suggested by $\delta^{18}\text{O}_{\text{mar}}$. The most likely explanation for that discrepancy is that timescale errors in the early intervals of the records (ice core and deep-sea sediment) are even larger than reported. For lag estimations between Vostok's CO_2 and ice-volume records, especially in the early interval, Vostok's $\delta^{18}\text{O}_{\text{air}}$ is probably a better global ice-volume indicator than $\delta^{18}\text{O}_{\text{mar}}$ because the advantage of its high stratigraphic accuracy outweighs its limitations as a proxy.

Short-term lag changes between Vostok's CO_2 and ice volume could not be estimated reliably with a running window as above. The poorer proxy/timescale quality of $\delta^{18}\text{O}_{\text{air}}/\delta^{18}\text{O}_{\text{mar}}$ would necessitate too broad a window. However, the “outlier behaviour” (Fig. 3) points to a short-term lag change after Termination II (see above).

5. Conclusions

This study has estimated the phase relations (leads/lags) of Vostok's CO_2 record relative to air temperature and global ice volume over the last 420 ka, extending the range of previous phase determinations by about 200 ka. Lagged GLS regression proved to be an efficient and precise estimation technique because it uses all data, and recognizes persistence inherent in the data. Bootstrap resampling allowed account to be taken of measurement and timescale errors.

On long timescales, variations in Vostok's CO_2 record lag behind those of its air-temperature record (δD) by 1.3 ± 1.0 ka, and lead over global ice-volume variations (derived from Vostok's $\delta^{18}\text{O}_{\text{air}}$ and marine $\delta^{18}\text{O}_{\text{mar}}$) by 2.7 ± 1.3 ka. Significant short-term changes in lag time occurred not only subsequent to glacial Termination II, but also subsequent to Termination III.

A summary of the results of this study is shown in Fig. 6. As regards causal explanations of Late Pleistocene glacial cycles, it has to be considered that Vostok's air temperature (δD) represents, at best, the Southern Hemisphere. Blunier et al. (1998) estimated that Greenland temperature variations lag behind those of Vostok by 1–2.5 ka over the period 47–23 ka. Thus, the geological relationships between variations in atmospheric CO_2 content, global temperature and ice volume are quite

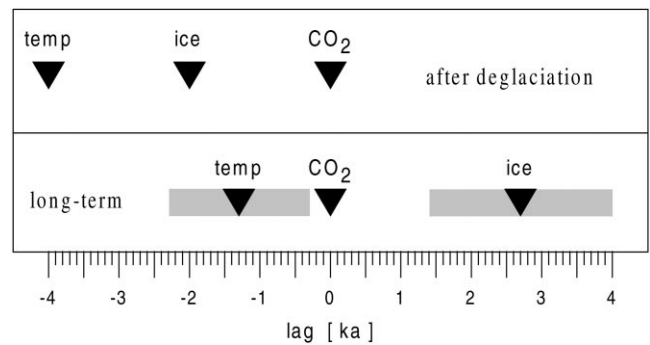


Fig. 6. Summary of results: estimated lags among atmospheric CO_2 content, Southern Hemisphere air temperature and global ice volume (derived from $\delta^{18}\text{O}_{\text{air}}$ and $\delta^{18}\text{O}_{\text{mar}}$). A negative lag value means a lead over CO_2 . In case of long-term climate (last 420 ka), the estimation uncertainties ($1 - \sigma$) are given as shaded bars. Subsequent to a deglaciation (Terminations II and III), for a short period a different phase relation prevails. In the upper panel, the lag between CO_2 and ice volume is rather uncertain; it may be more negative than the lag between CO_2 and temperature.

complicated in the Late Pleistocene. However, the phase relations identified in this study (Fig. 6) should help to constrain further the set of feasible scenarios as outlined, for example, by Broecker and Henderson (1998, Table 1 therein).

Note added in proof

Recently Shackleton (2000) argued that $\delta^{18}\text{O}_{\text{air}}$ has actually a better ice-volume proxy quality than $\delta^{18}\text{O}_{\text{mar}}$. Constructing a new, tuned Vostok timescale and using phase spectral estimations, he found that variations in atmospheric CO_2 , Vostok air temperature, and orbital eccentricity, at 100 ka period, were nearly synchronous over the past 420 ka and lead over ice-volume variations by 14 ± 2.5 (1 sigma) ka. As regards the results of the present study, his estimation uncertainty is too high to detect the lead of temperature relative to CO_2 variations (Section 3.1) whereas his estimated lag of ice-volume variations, though of the same sign as estimated here (Sections 3.2 and 3.3), is clearly larger. This discrepancy might be resolved considering that (1) Shackleton's phase estimations were made relative to ETP (a mixture of eccentricity, tilt and precession)—thus, the high stratigraphic accuracy of $\delta^{18}\text{O}_{\text{air}}$ relative to CO_2 (Section 3.3) was not used; (2) the uncertainty reported by him seems not to take into account timescale inaccuracies; (3) he used an atmospheric turnover time of 1.0 ka (we used 2.0 ka, Section 4); and (4) the lag estimated here is an *average* over the periods of variation.

Acknowledgements

I thank A.L. Berger and M. Schulz for the discussions. Thanks are expressed for the careful review comments

which were particularly helpful for improving the clarity of presentation. Release of the data used is gratefully acknowledged. The major part of the present study was carried out while the author was Marie Curie Research Fellow (EU-TMR grant ERBFMBICT 971919) at the Institute of Mathematics and Statistics, University of Kent, Canterbury, UK.

References

- Barnola, J.-M., Pimienta, P., Raynaud, D., Korotkevich, Y.S., 1991. CO₂-climate relationship as deduced from the Vostok ice core: a re-examination based on new measurements and on a re-evaluation of the air dating. *Tellus B* 43, 83–90.
- Bassinot, F.C., Labeyrie, L.D., Vincent, E., Quidelleur, X., Shackleton, N.J., Lancelot, Y., 1994. The astronomical theory of climate and the age of the Brunhes–Matuyama magnetic reversal. *Earth and Planetary Science Letters* 126, 91–108.
- Bender, M., Sowers, T., & Labeyrie, L., 1994. The Dole effect and its variations during the last 130,000 years as measured in the Vostok ice core. *Global Biogeochemical Cycles* 8, 363–376.
- Berger, A., Loutre, M.F., 1991. Insolation values for the climate of the last 10 million years. *Quaternary Science Reviews* 10, 297–317.
- Blunier, T., Chappellaz, J., Schwander, J., Dällenbach, A., Stauffer, B., Stocker, T.F., Raynaud, D., Jouzel, J., Clausen, H.B., Hammer, C.U., Johnsen, S.J., 1998. Asynchrony of Antarctic and Greenland climate change during the last glacial period. *Nature* 394, 739–743.
- Broecker, W.S., Henderson, G.M., 1998. The sequence of events surrounding Termination II and their implications for the cause of glacial–interglacial CO₂ changes. *Paleoceanography* 13, 352–364.
- Broecker, W.S., van Donk, J., 1970. Insolation changes, ice volumes, and the O¹⁸ record in deep-sea cores. *Reviews of Geophysics and Space Physics* 8, 169–198.
- Efron, B., Tibshirani, R.J., 1993. *An Introduction to the Bootstrap*. Chapman & Hall, London.
- Hays, J.D., Imbrie, J., Shackleton, N.J., 1976. Variations in the Earth's orbit: Pacemaker of the ice ages. *Science* 194, 1121–1132.
- Herrmann, E., 1997. Local bandwidth choice in kernel regression estimation. *Journal of Computational and Graphical Statistics* 6, 35–54.
- Imbrie, J., Hays, J.D., Martinson, D.G., McIntyre, A., Mix, A.C., Morley, J.J., Pisias, N.G., Prell, W.L., Shackleton, N.J., 1984. The orbital theory of Pleistocene climate: Support from a revised chronology of the marine $\delta^{18}\text{O}$ record. In: Berger, A., Imbrie, J., Hays, J., Kukla, G., Saltzman, B. (Eds.), *Milankovitch and Climate, Part II*. D. Reidel, Dordrecht, pp. 269–305.
- Li, X.S., Berger, A., Loutre, M.F., 1998. CO₂ and northern hemisphere ice volume variations over the middle and late Quaternary. *Climate Dynamics* 14, 537–544.
- Malaizé, B., Paillard, D., Jouzel, J., Raynaud, D., 1999. The Dole effect over the last two glacial–interglacial cycles. *Journal of Geophysical Research* D104, 14 199–14 208.
- Martinson, D.G., Pisias, N.G., Hays, J.D., Imbrie, J., Moore, T.C., Shackleton, N.J., 1987. Age dating and the orbital theory of the ice ages: development of a high-resolution 0 to 300,000-year chronostratigraphy. *Quaternary Research* 27, 1–29.
- Mudelsee, M., 2000. Ramp function regression: a tool for quantifying climate transitions. *Computers and Geosciences* 26, 293–307.
- Petit, J.R., Jouzel, J., Raynaud, D., Barkov, N.I., Barnola, J.-M., Basile, I., Bender, M., Chappellaz, J., Davis, M., Delaygue, G., Delmotte, M., Kotlyakov, V.M., Legrand, M., Lipenkov, V.Y., Lorius, C., Pépin, L., Ritz, C., Saltzman, E., Stievenard, M., 1999. Climate and atmospheric history of the past 420,000 years from the Vostok ice core, Antarctica. *Nature* 399, 429–436.
- Raynaud, D., Jouzel, J., Barnola, J.M., Chappellaz, J., Delmas, R.J., Lorius, C., 1993. The ice record of greenhouse gases. *Science* 259, 926–934.
- Robinson, P.M., 1977. Estimation of a time series model from unequally spaced data. *Stochastic Processes and their Applications* 6, 9–24.
- Sen, A., Srivastava, M., 1990. *Regression Analysis*. Springer, New York.
- Shackleton, N.J., 2000. The 100,000-year Ice-Age cycle identified and found to Lag temperature, carbon dioxide, and orbital eccentricity. *Science* 289, 1897–1902.
- Sowers, T., Bender, M., Raynaud, D., Korotkevich, Y.S., Orchardo, J., 1991. The $\delta^{18}\text{O}$ of atmospheric O₂ from air inclusions in the Vostok ice core: timing of CO₂ and ice volume changes during the penultimate deglaciation. *Paleoceanography* 6, 679–696.
- Tukey, J.W., 1977. *Exploratory Data Analysis*. Addison-Wesley, Reading, MA.